Biochimica et Biophysica Acta, 1106 (1992) 264–272

BBAMEM 75617

An electrophysiological and spectroscopic study of the properties and structure of biological calcium channels. Investigations of a model ion channel

David G. Reid [a], Lesley K. MacLachlan [a], Colin J. Salter [a], Martin J. Saunders [a], Steven D. Jane [b], Anthony G. Lee [b], E. John Tremeer [c] and Stephen A. Salisbury [c]

[a] *Analytical Sciences Department, Chemistry Support, SmithKline Beecham Pharmaceuticals Ltd., Welwyn (UK),* [b] *Department of Biochemistry, University of Southampton, Southampton (UK) and* [c] *Pharmacia LKB Biochrom, Science Park, Cambridge (UK)*

(Received 30 January 1992)

Key words: Electrophysiology; Spectroscopy; Calcium ion channel; Ion channel

The N- and C-terminally protected peptide *N*-acetyl-Asp-Phe-Ala-Asn-Arg-Val-Leu-Leu Ser-Leu-Phe-Thr-Ile-Glu-Met-Leu-Leu-Lys-Met-Tyr-Gly-Leu-NH_2, closely based on the sequence of the putative S2 membrane spanning helix of domain II of the dihydropyridine receptor calcium channel of the T-system of skeletal muscle, residues 465–486 (Tanabe et al. (1987) Nature 328, 313–318) has been synthesised. Conductance measurements in planar lipid bilayers show that the peptide is capable of inducing the transmembrane passage of calcium and barium ions, in preference to monovalent cations. No anion conductance is observed. ^{1}H-NMR spectroscopy demonstrates that in an amphilic solvent, methanol, the peptide forms highly stable structures characterised by very slow exchange with solvent of peptide N-H protons. Double-quantum filtered phase-sensitive COSY shows that, on the basis of NH-CH_α scalar coupling constants, most peptide torsion angles are appropriate to an overall α-helical conformation; the presence of some α-helix is also supported by CD measurements. Most side-chain connectivities have been identified in a DIPSI-TOCSY experiment. This evidence has been used to construct a low-resolution model of the ion-conducting channel of the muscle T-system dihydropyridine receptor from the sequences of the four homologous putative channel-lining stretches. It is characterised by an association of acidic residues at the putative extra-membranous face of the channel, followed by a predominantly hydrophobic band. The next prominent feature of the model is an ordered array of four acidic residues (glutamates 100, 478, 846 and 1164), followed by four lysines (104, 482, 850 and 1168) which may play a gating role.

Introduction

Transmembrane ion channels are important pharmacological targets; their three-dimensional conformations are currently inaccessible in atomic detail by any high resolution structure determination technique. Drugs which act on calcium channels are of proven clinical efficacy in conditions such as cardiac fibrillation and hypertension [1,2], and their uses in other presently intractable conditions, such as treatment of post-ischaemic reperfusion damage, holds great promise. Current ideas about the structure of proteinaceous ion channels in membranes support the concept, based on primary structural hydrophobicity mapping and limited crystallographic data, of bilayer-spanning lipophilic α-helices supporting extra-membraneous globular domains. The latter probably contain the drug binding loci. The precise geometry of these putative membrane spanning α-helices is potentially relatively easily definable by contemporary high resolution techniques, in contrast to the extramembraneous domains, although their chemical synthesis and purification can be challenging. The former represent valuable starting points for molecular modelling of the entire structure of ion channels. The primary structures of several types of calcium channel have been determined [3–8]. They show homologies with some other cation channels, and as such represent useful test cases for a generalised approach to the elucidation of the three-dimensional structure of ion channels, based on a combination of predictive and physico-chemical structure determination methods.

We have synthesised a 22-residue peptide conforming to the S2 helix of domain II of the skeletal muscle dihydropyridine receptor, predicted to be one of the four amphiphilic channel-lining helices commencing at Asp-465 [3] and confirmed that it is able to self assem-

Correspondence: D.G. Reid, Analytical Sciences Department, SmithKline Beecham Pharmaceuticals Ltd. The Frythe, Welwyn, Herts AL6 9AR, UK.

ble to form functional channels in model black lipid membranes (BLM's) which are highly specific for alkali earth cations. Preliminary ^{1}H-NMR experiments in an amphiphilic solvent, methanol, show that the peptide adopts a stable, oligomeric and probably α-helical conformation; the presence of some α-helical structure is also supported by CD measurements while molecular modelling of all four putative channel-lining helices suggests some important mechanistic features of ion transmission and channel gating.

Materials and Methods

Peptide synthesis

The N- and C-terminally blocked sequence *N*-acetyl-Asp-Phe-Ala-Asn-Arg-Val-Leu-Leu-Ser-Leu-Phe-Thr-Ile-Glu-Met-Leu-Leu-Lys-Met-Tyr-Gly-Leu-NH_2 was synthesised according to the solid phase Fmoc method [9] using a continuous flow apparatus (Pharmacia-LKB 4170) and pentafluorophenyl esters in combination with *N*(1)-hydroxybenzotriazole for peptide coupling. The carboxyl terminal residue was attached to the polyamide-kieselguhr composite synthesis support via an acid-labile, amide-generating linker (Pharmacia-LKB 'Ultrosyn C'). Successive coupling reactions were carried out under CDM monitoring [10], with feedback control of the time allowed for each reaction. Cleavage and deprotection of the product was effected by treatment with aqueous trifluoroacetic acid (TFA) (95% v/v) containing ethanedithiol as a scavenger for carbocations. The peptide was recovered by evaporation and freed from low molecular weight contaminants by solvent extraction of the redissolved material and its composition confirmed by amino acid analysis. Its molecular weight was confirmed by FAB mass spectrometry, which in positive mode showed a peak corresponding to $M + Na^+$ at 2608 atomic mass units.

Electrophysiological studies

Phospholipids were purchased from Avanti Polar Lipids, AL, USA and from Lipid Products, Surrey, UK. The salts used were of Analar grade purchased from the Sigma Chemical Company Ltd.

Bilayers were formed from decane solutions of phosphatidylethanolamine and phosphatidylserine mixed in a 1:1 molar ratio to produce a final lipid concentration of 4 mg ml^{-1}. When formed, the bilayer separated two aqueous chambers, one of which, designated *cis*, could be voltage clamped at a range of holding potentials relative to ground while the other chamber, designated *trans*, was held at virtual ground. The *cis* chamber consisted of a polycarbonate cup containing an aperture of 300 μm diameter across which bilayers with capacitances of 1–2 nF were painted. The *trans* chamber was made from Perspex. Current flow through the bilayer was monitored using a patch and cell clamp amplifier (Biologic RK300) as a current-to-voltage converter via glass salt bridges in series with Ag/AgCl electrodes. The output of the amplifier was displayed on an oscilloscope, digitised using a pulse code modulator (Biologic PCM-modified Sony PCM 701ES) and stored on videotape [11,12] for analysis at a later date. No conductance was observed in the absence of peptide.

Peptide (0.1 mg) was dissolved in 1 ml of methanol and aliquoted into ten glass vials. The methanol was then evaporated under nitrogen and the vials sealed and stored at −20°C until required. Prior to experimentation 0.5 ml of methanol was added to a vial to give a peptide concentration of 0.02 mg ml^{-1}. Peptide was added to the *cis* chamber of the bilayer set-up and stirred until fusion occurred with the bilayer. The final concentration of peptide in the *cis* chamber was 0.1 μg to 0.2 μg ml^{-1}. Following incorporation any unfused peptide was perfused out of the *cis* chamber. Experiments were carried out at room temperature (20 to 25°C and at pH 7.4) with salt solutions as indicated.

Data stored on videotape were converted back to an analogue signal via the output channel of the PCM and low-pass filtered at a corner frequency of 300 Hz (Frequency Devices 902LP Filter). Files were created for computer analysis by digitising filtered data at 5KHz from videotape runs of 40–60 s and analysed using a commercial software package (Satori V.3.01, Intracel Ltd.). Fitting of lifetime data was by the maximum likelihood method. A correction for missed events was applied by setting a 'correction' parameter to the minimum resolvable lifetime, 5 ms in these experiments.

NMR spectroscopy

5 mg of peptide, which is insoluble in water or aqueous SDS, was dissolved in 0.4 ml CD_3OH or CD_3OD (Aldrich) to give rise to a viscous apparently gel-like solution, which, however, produced well resolved ^{1}H-NMR spectra.

Variable temperature experiments were performed on a Bruker AM360 spectrometer. Free induction decays (FID's) were acquired with 16K digitisation, a sweep width of 3968 Hz (11 ppm) with 256 scans and at intervals of 5°C between 25°C and 50°C.

Two-dimensional (2-D) experiments were performed on a Bruker AMX400 spectrometer. Typically, 512 FID's were acquired at 37°C with 2K digitisation, a sweep width of 4400 Hz (11 ppm), with 32 scans per increment. A DIPSI mixing sequence [13] was used in the total correlation spectrum (TOCSY) [14,15] pulse sequence. Matrices were processed using a sine-bell apodisation function in each domain; the datasets were zero-filled to 4K × 1K prior to Fourier transformation.

Circular dichroism

The solution used for NMR was diluted approx. 25-fold with CH_3OH (BDH Spectrosol) and then centrifuged to remove suspended oily droplets. The concentration of the resulting solution was determined from the tyrosine absorbance at 278 nm.

CD spectra were recorded at approximately 25°C on a JASCO J-600 spectropolarimeter, using a sensitivity of 20 millidegrees, 2.0 nm band width, 4 s time constant and 10 nm/min scan speed, with the solution in a 0.02 cm pathlength cylindrical cell. In order to check that light scattering was not causing distortion, spectra were recorded with the cell in its normal position and also with it close to the photomultiplier.

Results

Planar bilayer conductance measurements

No chemical or electrical gradients were required to induce fusion of the peptide bilayers, and incorporation occurred in a range of salt solutions. Final *cis* chamber peptide concentrations of 0.1 μg ml^{-1} or above were necessary to obtain fusion and channel-like activity. The limited amount of peptide precluded repetition of certain experiments to produce more accurate results.

Fig. 1A illustrates the square-wave nature of conductance fluctuations observed in symmetrical *cis*/*trans* 5 mM $CaCl_2$/50 mM choline chloride/10 mM Hepes-Tris (pH 7.4), following fusion of peptide with a bilayer. The conductance of the channel shown was 13 pS at a holding potential of + 100 mV although the recording shown in Fig. 1A is typical. Conductance estimates determined from channels in identical ion solutions were sometimes found to vary between experiments. Fig. 2 shows the mean current/voltage relationship for recordings ($n = 4$) of peptide channels in symmetrical 5 mM $CaCl_2$/50 mM choline chloride/10 mM Hepes-Tris (pH 7.4). The mean conductance of the channels, which displayed similar conductance states, was 10 pS, indicating the passage of $3.12 \cdot 10^6$ ions per s.

Fig. 3 illustrates amplitude and lifetime analysis for the channels depicted in Fig. 1A and which was used to construct Fig. 2. The conductance of the channel at this holding potential (+ 100 mV) was 13 pS. The open and closed times seen with this channel were typical of those observed for all other recordings in symmetrical 5 mM $CaCl_2$/50 mM choline chloride/10 mM Hepes-Tris (pH 7.4). Computer analysis of open and closed times fitted to double exponentials with $\tau_1 = 2.1$ and $\tau_2 = 181$ ms and an amplitude ratio of fast to slow component of 3.8 for open channel state and $\tau_1 = 2.2$ and $\tau_2 = 195$ ms and an amplitude ratio of fast to slow component of 2.7 for the dried channel state.

To demonstrate that calcium was the ion being transported by the peptide channel a protocol utilising (asymmetrical) calcium as the only mobile ion species was adopted [15]. Under these conditions conductance fluctuations were seen (Fig. 1B) whereas when conditions were altered so that chloride was the only potential mobile ion species no such fluctuations were observed.

To show that other divalent ions could be transported by the peptide channel calcium ions were replaced with barium ions. This resulted in an increase in channel conductance from 13 pS to an average conductance of 25 pS. The addition of lanthanum chloride to both *cis* and *trans* chambers to final concentrations of 10, 20 and 30 μM produced no obvious changes in

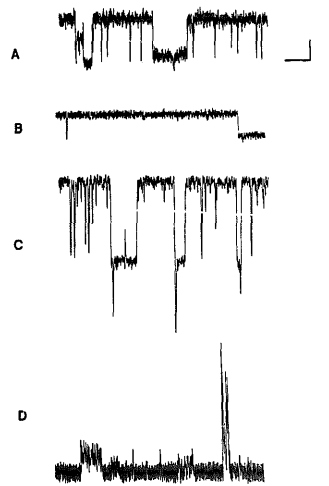

Fig. 1. (A) Peptide channel activity in symmetrical 5 mM $CaCl_2$/50 mM choline chloride/10 mM Hepes-Tris (pH 7.4). The bilayer was clamped at + 100 mV. (B) Conductance fluctuations seen with *cis* 250 mM Hepes-Tris (pH 7.4) and *trans* 53 mM Ca^{2+}/250 mM Hepes-Tris (pH 7.4). Bilayer was clamped at + 100 mV. This trace has been inverted relative to the other traces. (C) Multiple openings observed in symmetrical 5 mM $CaCl_2$/50 mM choline chloride/10 mM Hepes-Tris (pH 7.4). Bilayer was clamped at + 120 mV. (D) Channel activity in symmetrical 100 mM CsCl/10 mM Hepes-Tris (pH 7.4). The bilayer was clamped at + 100 mV. The lowest open level shown was the most common and was used to construct the *I-V* relationship. Channel openings are depicted as upward deflections. The scale bars are 1 pA and 500 ms for all traces. Original data was low pass filtered at 300 Hz and digitised at 5 kHz prior to analysis.

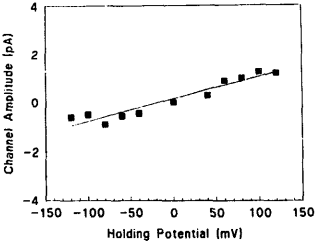

Fig. 2 Mean single-channel current/voltage relationship for the peptide channel after incorporation into bilayers immersed in symmetrical 5 mM $CaCl_2$/50 mM choline chloride/10 mM Hepes-Tris (pH 7.4). Each point is the mean of four determinations, each determination being the mean of channel amplitudes measured at the stated holding potential in separate experiments. Mean channel conductance was 10 pS.

channel conductance or open/closed times. Ruthenium red also failed to alter channel activity.

Occasionally, it appeared that sufficient peptide incorporated into the BLM to give multiple channels, giving rise to multiple simultaneous openings (Fig. 1C); when present these higher conductance events appeared with increasing frequency as the value ($\pm$) of the holding potential across the bilayer was increased.

The peptide channel was also found to be capable of conducting monovalent cations. When caesium was the mobile ion species channel activity was also observed (Fig. 1D). Activity was noisier and more erratic when compared to that seen with divalent ions and channels spent less time in the open-state than when conducting divalent ions. Variation of ion solutions used showed this was a constant feature over a range of ionic strengths. The channel showed a conductance of approximately 15 pS in symmetrical caesium chloride (100 mM). The channel only showed activity at positive holding potentials.

NMR determinations

Fig. 4 summarises the behaviour of the peptide NH protons in methanol. Fig. 4A shows the aromatic and NH spectral region of the ^1H spectrum of the peptide in CD_3OD (methanol-d_4), obtained about half an hour after dissolution; it is remarkable for the persistence of a number of N-H signals which would normally exchange rapidly with solvent deuterium. The corresponding ^1H spectra of the peptide in CD_3OH (methanol-d_3) at ambient temperature and 50°C are shown in Figs. 4B and C, respectively; even at the higher temperature most of the potentially exchangeable peptide NH signals show no evidence of intermediate or fast exchange with solvent, which would be manifest as signal broadening accompanied by upfield shifting or disappearance.

Fig. 5 displays the region of the DIPSI-TOCSY spectrum of the peptide in methanol-d_3 at 37°C containing NH-CHα and subsequent crosspeaks. The entire spin systems of several of the constituent amino acid residues can be traced out, and these connectivities are marked on the figure. It was also possible to estimate a number of NH-CHα three-bond coupling constants from a double-quantum filtered COSY experiment (results not shown). These were all in the 3–5 Hz range, which is consistent with the adoption of a predominantly α-helical backbone secondary structure.

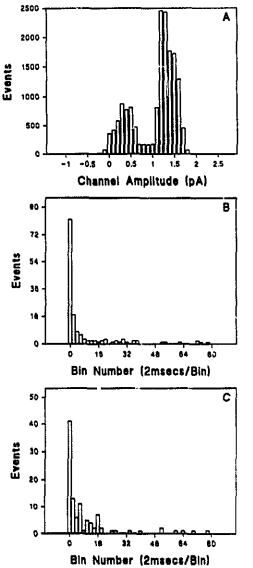

Fig. 3. (A) Amplitude histogram of channel openings observed in symmetrical 5 mM $CaCl_2$/50 mM choline chloride/10 mM Hepes-Tris (pH 7.4) when held at +100 mV. Bins were 0.2 pA. Gaussian fits to the data revealed a mean closed channel level of 0.38 pA and a mean open channel level of 1.68 pA, giving a mean channel amplitude of 1.3 pA at +100 mV, corresponding to a conductance of 13 pS. (B) Open time histogram for the channel observed in (A). (C) Closed time histogram for the channel observed in (A).

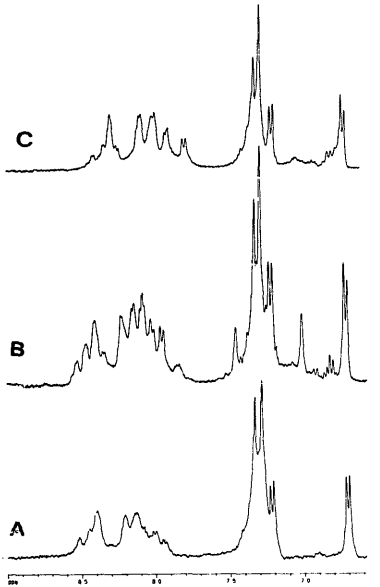

Fig. 4. The lowfield region of 360 MHz ^1H spectra of 5.5 mg of the peptide in (A) methanol-d_4 at 25°C; (B) methanol-d_3 at 25°C and (C) methanol-d_3 at 50°C.

CD determinations

The obstacles to total structure determination by NMR presented by limited quantities of peptide and its viscosity in solution led us to use a complementary technique, CD spectroscopy, to confirm the NMR-based deductions of α-helix formation. Accordingly, Fig. 6 shows the CD spectrum of a methanolic solution of the peptide at a concentration which corresponds to 3.7 mM amino acid residues, ie 0.17 mM peptide. Evidence for the presence of α-helical structures is given by the positive Cotton effect below 200 nm and the negative effects at approx. 208 nm and approx. 220 nm, although the latter manifests as a shoulder due to the presence of some proportion of other structures.

Discussion

The small size, and hydrophobicity, of the peptide used implied that only true bilayers would be of the right dimensions to allow the peptide to incorporate, span the bilayer and form functional ion channels. With this in mind and given that bilayers often 'thicken' during the course of an experiment the approx. 10% success rate achieved in the BLM experiments was comparable or better than that obtained for many preparations of channels from natural sources.

Our 22 amino acid peptide incorporated into bilayers to form well defined ion channels with specific ion permeabilities and lifetime characteristics. The peptide channels showed the typical square-wave conductance fluctuations characteristic of transmembraneous protein channels as they shift between their conductive and non-conductive states, features also reported when a synthetic 22 amino acid peptide based on the voltage-sensitive sodium channel was incorporated into bilayers [17] and when a 21 amino acid peptide was incorporated by Lear et al. [18]. When *trans* calcium was the only mobile ion species present in the bathing media channels appeared to be in the open/conducting state for much of the time, closing for only brief periods. Unfortunately only limited data were gained under these conditions, although they were sufficient to demonstrate clearly the channel's ability to conduct calcium.

With calcium or barium as the mobile ion species well defined channels were often observed. The tendency for indigenous transmembrane calcium channels to be permeable to barium ions and for single-channel conductances to be greatest with this ion as the charge carrier were features also displayed by the peptide channel. Unlike other calcium channels which are blocked by lanthanum ions in micromolar concentrations the peptide channel was not affected by the addition of up to 30 μM $LaCl_3$ (*cis* and *trans*). The apparent failure to block the channel may, perhaps, have been a consequence of the peptide assembling to form a pore that was larger than that normally associated with membrane calcium channels or, that lanthanum ions may not depend on their size to accomplish a block but use their charge to bind to, and effect changes in, other parts of the channel protein. Oiki et al. [16] found that a 22-mer, based on the putative membrane spanning region of the voltage-sensitive sodium channel, exhibited conductances similar to those recorded for the actual sodium channel. The conductance of the synthetic peptide channel in 50 mM barium was comparable to that of the dihydropyridine receptor calcium channel (approx. 25 pS; [19]) (Figs. 1A and 2).

The peptide channel was able to conduct caesium (Fig. 1D) but in comparison to the divalent ions tested the appearance of the conductance transitions were very different. Instead of typical square-wave transitions from conducting to non-conducting states transitions occurred in rapid bursts interposed with compar-

atively long closed periods. This feature was not found to be an ionic strength phenomenon. The channel was only active at positive holding potential perhaps reflecting an asymmetrical distribution of peptide within the bilayer.

Molecular modelling of the calcium channel

Our NMR and CD results demonstrate that the peptide is able to form stable structures in an amphiphilic solvent, which are probably α-helical. We accordingly decided to attempt to model the environment of the ion-conductance channel itself by constructing the four putative channel lining helices, using the COSMIC modelling programme [20] corresponding to the S2 helices of domains I to IV (residues 87–108, 465–486, 836–854 and 1151–1172) of the sequence of Tanabe et al. [3]. As our high resolution structure determination studies are still at a preliminary stage, the modelling of the channel was performed manually and interactively on an Evans and Sutherland PS-300 using idealised α-helical backbone torsion angles and fully extended side chain conformations. We do not consider it appropriate at this stage to undertake any computational modelling, given that such important factors as the relative juxtapositioning of the four helices, impossible to predict from hydropathy profiling, has yet to be established experimentally.

The four helices were aligned with their helical axes parallel, as opposed to antiparallel (mutual repulsion of the considerable electric dipoles associated with helices could be compensated for in the holoprotein by neighbouring helices) and separated by suitable van

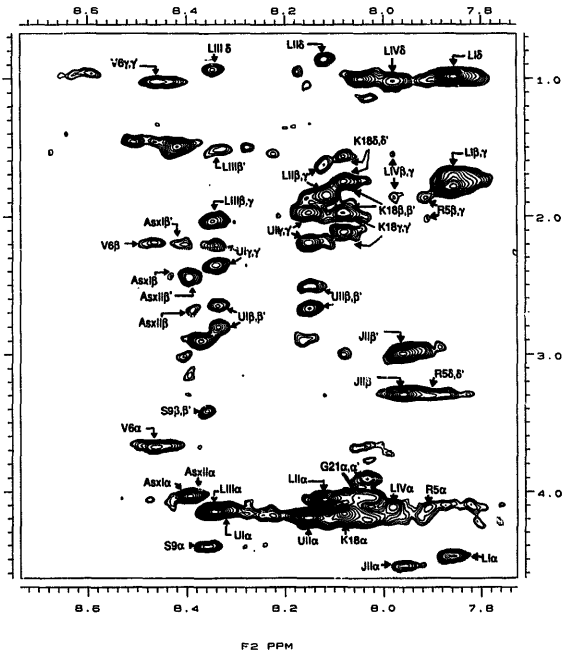

Fig. 5. A region of the 400 MHz DIPSI-TOCSY spectrum of 5.5 mg of the peptide in methanol-d_3, at 37°C, displaying NH to CH_α and subsequent intra-residue through-bond couplings. As many spin systems as possible have been identified and these are indicated on the figure. Spin system types are referred to by the convention of Redfield and Dobson [28].

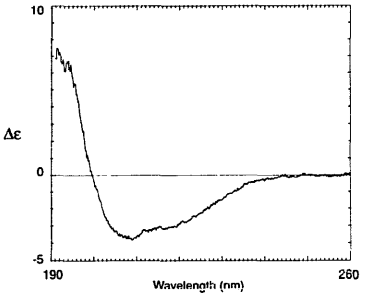

Fig. 6. Far-UV CD spectrum of the peptide (0.17 mM) in methanol at approx. 25°C. The spectrum was converted to $\Delta\varepsilon$ using the concentration of amino acid residues (3.7 mM).

der Waals' distances. This parallel alignment is obligatory if the transmembrane topology of the protein suggested by hydropathy profiling is correct. As far as possible relative rotation of helices was contrived so as to place as many charged residues as possible along the lining of the channel. The model, various aspects of which are shown in stereo in Fig. 7, clearly only represents a starting point in understanding calcium channel structure, as it displays several unsatisfactory features such as the close mutual proximity of several negatively charged side chains (Glu-100, -478, -846 and -1164), and of several positively charged side chains (Lys-104, -482, -850 and -1168). We believe, however, that it does suggest several broad structural characteristics which should prove useful in relating the structure of ion channels to their function (Ref. 21 and references cited therein).

Firstly, the putatively extracellular mouth of the channel is modelled to comprise several acidic or polar residues (Glu-87 and Glu-90 on IS2, Asp-465 and Asn-468 on IIS2, Asp-836 on IIIS2, and Asp-1151 and Asn-1154 on IVS2) which a parallel alignment of α-helices brings into a loose association. It may be this feature which controls the ion-capture which is a prerequisite for transport. Deeper into the channel is a prominent band of predominantly hydrophobic amino acids, phenylalanines and leucines, which may play a role in modulating the hydration state of the transmitted ion. A third feature suggested by the simple juxta-

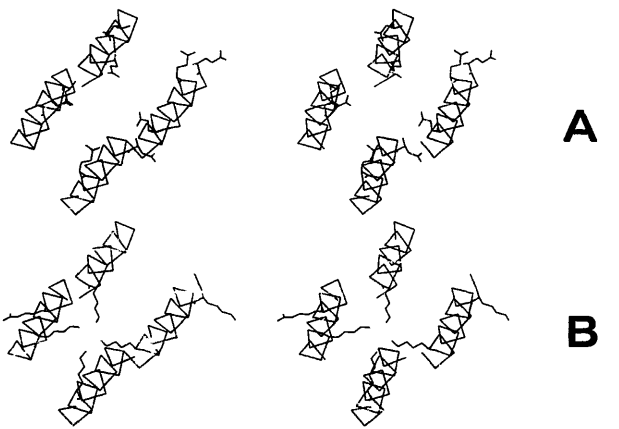

Fig. 7. Stereo drawings of an initial structural model of a calcium channel, assembled as described in the text. The sequences of the four helices shown correspond to sequences 87-EKLEYFFLTVFSIEAAMKIIAY (right hand side of each drawing), 465-DIANRVLLSLFTIEMLLKMYGL (left hand side), 836-DIAFTSVFTVEIVLKMTYY (top) and 1151-DILNVAFTIIFTLEMILKLLAF (bottom). For the sake of clarity only the side chains of negatively charged residues (aspartates and glutamates) are portrayed in A. Similarly B, C, D and E depict the side chains of positive, aromatic, aliphatic and polar uncharged residues, respectively. The extracellular mouth of the channel is to be visualised at the top right hand corner of each structural presentation.

positioning of parallel α-helices is an ordered band of four negative side chains (Glu-100, -478, -846 and -1164) creating a potentially high affinity chelating structure. Finally, four potentially positively charged side chains (Lys-104, -482, -850 and -1168) protruding into the channel may play a role as a gating mechanism whereby channel conductance is linked via allosteric effects to the free energy changes consequent on agonist binding, or alterations in transmembrane potential [22]. The influence of these ionisable residues on each other's protonation states is difficult to quantify [23]. These four glutamate and four lysine residues are strongly conserved in all mammalian calcium channels sequenced to date [3–8]. The presence of the latter close to the distal end of the channel may have implications for inactivation mechanisms for potassium channels, proposed on the basis of site directed mutagenesis, involving channel plugging by a predominantly positively charged N-terminal domain [24,25]. Similarly the hypothesis that the functional entity of some potassium channels is comprised of an aggregation of β-hairpin structures rather than amphiphillic helices [26] requires confirmation by high resolution structural techniques. The proposed calcium pore, and those of the other sequences already cited, is also virtually devoid of any proline residues, suggested as being obligatory components of at least some ion channels [27]. Most of the channel proteins investigated by these last authors are specific for alkali metal cations, or halide anions; it is possible that these larger hydrated

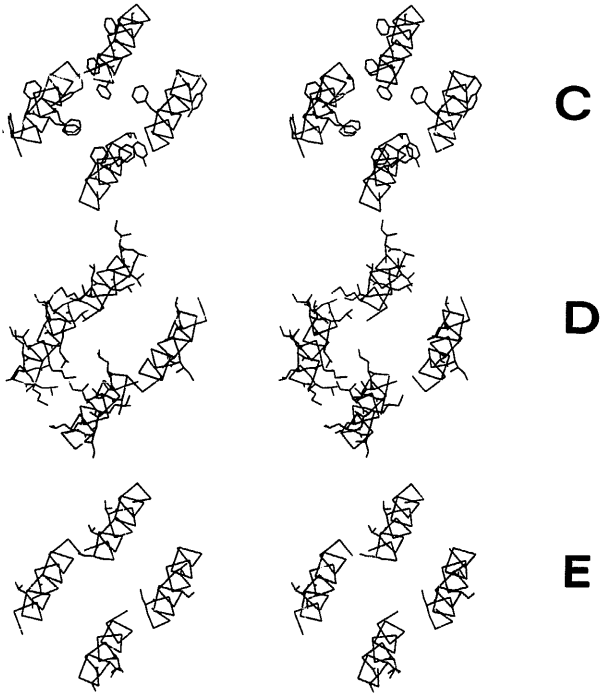

ions demand the greater flexibility conferred by the presence of proline in the pore sequence, which is not obligatory for the smaller alkaline earth cations. Interestingly, none of the several serine and threonine residues in the four sequences is modelled to be directed into the interior of the channel. They may play a role in maintaining channel integrity, rather than being directly involved in conductance.

Conclusions

It has been shown that a 22-residue peptide based on the sequence of one of the putative channel-lining α-helices of a membrane bound calcium channel does conduct divalent cations in a specific manner. CD and ^{1}H-NMR studies in an amphiphilic solvent also indicate that it forms stable structures which appear to have α-helical content. Initial molecular modelling studies based on hydropathy profiling and some assumptions of overall channel structure are currently being extended, using through-space NOE connectivities and further data from Fourier-transform infra-red and CD, to understanding the structure of the calcium channel holoprotein.

Acknowledgements

We thank our colleagues Drs. Jackie Hunter, Tom Brown and Ted Pepper for their interest in this work, Dr. Neville Haskins for FAB mass spectrometry, and the SERC for financial support (to A.G.L.).

References

1 Rang, H.P. and Dale, M.M. (1987) Pharmacology, pp. 248–250. Churchill Livingstone, London.
2 Needleman, P., Corr, P.B. and Johnson, E.M., Jr. (1985) The Pharmacological Basis of Therapeutics, 7th Edn., (Gilman, A.G., Goodman, L.S., Rall, T.W. and Murad, F., eds.), pp. 816–822, MacMillan, Basingstoke.
3 Tanabe, T., Takeshima, H., Mikami, A., Flockerzi, V., Takahashi, H., Kangawa, K., Kojima, M., Matsuo, H., Hirose, T. and Numa, S. (1987) Nature 328, 313–318.
4 Mikami, A., Imoto, K., Tanabe, T., Niidome, T., Mori, Y., Takeshima, H., Narumiya, S. and Numa, S. (1989) Nature 340, 230–233.
5 Takeshima, H., Nishimura, S., Matsumoto, T., Ishida, H., Kangawa, K., Minamino, N., Matsuo, H., Ueda, M., Hanaoka, M., Hirose, T. and Numa, S. (1989) Nature 339, 439–445.
6 Biel, M., Ruth, P., Bosse, E., Hullin, R., Stuhmer, W., Flockerzi, V. and Hoffman, F. (1990) FEBS Lett. 269, 409–412.
7 Koch, W.J., Ellinor, P.T. and Schwartz, A. (1990) J. Biol. Chem. 265, 17786–17791.
8 Mori, Y., Friedrich, T., Kim, M.-S., Mikami, A., Nakai, J., Ruth, P., Bosse, E., Hofmann, F., Flockerzi, V., Furuichi, T., Mikoshiba, K., Imoto, K., Tanabe, T. and Numa, S. (1991) Nature 350, 398–402.
9 Dryland, A. and Sheppard, R.C. (1988) Tetrahedron 44, 859–876.
10 Salisbury, S.A., Tremeer, E.J., Davies, J.W. and Owen, D.E.I.A. (1990) J. Chem. Soc. Chem. Commun., 538–540.
11 Bezanilla, F. (1985) Biophys. J. 47, 437–441.
12 Lamb, T.D. (1985) J. Neurosci. Methods 15, 1–13.
13 Shaka, A.J., Lee, C.J. and Pines, A. (1988) J. Magn. Reson. 77, 274–293.
14 Braunschweiler, L. and Ernst, R.R. (1983) J. Magn. Reson. 53, 521–528.
15 Davis, D.G. and Bax, A. (1985) J. Am. Chem. Soc. 107, 2820–2821.
16 Smith, J.S., Coronado, R. and Meissner, G. (1985) Nature 316, 446–449.
17 Oiki, S., Danho, W. and Montal, M. (1986) Proc. Natl. Acad. Sci. USA 85, 2393–2397.
18 Lear, J.D., Wasserman, Z.R. and DeGrado, W.F. (1988) Science 240, 1177–1181.
19 Reuter, H. and Porzig, H. (1989) in Ion Transport, (Keeling, D. and Benham, C., eds.) pp. 87–96 Academic Press, London.
20 Vinter, J.G., Davis, A. and Saunders, M.R. (1987) J. Computer Aided Mol. Design 1, 31–51.
21 Hladky, S.B. (1989) in Ion Transport (Keeling, D. and Benham, C., eds.), pp. 263–278, Academic Press, London.
22 Nowycky, M.C., Fox, A.P. and Tsien, R.W. (1985) Nature 316, 440–443.
23 Edmonds, D.T. (1989) in Ion Transport (Keeling, D. and Benham, C., eds.), pp. 279–292, Academic Press, London.
24 Hoshi, T., Zagotta, W.N. and Aldrich, R.W. (1990) Science 250, 533–538.
25 Zagotta, W.N., Hoshi, T. and Aldrich, R.W. (1990) Science 250, 568–571.
26 Yool, A.J. and Schwartz, T.L. (1991) Nature 349, 700–704.
27 Woolfson, D.N., Mortishire-Smith, R.J. and Williams, D.H. (1991) Biochem. Biophys. Res. Commun. 175, 733–7.
28 Redfield, C. and Dobson, C.M. (1988) Biochemistry 27, 122–136.